Activity and stability of bifunctional perovskite/carbon-based electrodes for the removal of antipyrine by electro-Fenton process

A. Cruz del Álamo [a], A. Puga [b], M.I. Pariente [a], E. Rosales [b], R. Molina [a], M. Pazos [b], F. Martínez [a,*], M.A. Sanromán [b,**]

[a] Department of Chemical and Environmental Technology, ESCET, Rey Juan Carlos University, 28933, Móstoles, Madrid, Spain
[b] CINTECX, Universidade de Vigo, Grupo de Bioingeniería y Procesos Sostenibles, Departamento de Ingeniería Química, Campus Lagoas-Marcosende, Vigo, 36310, Spain

HIGHLIGHTS

- Perovskite/carbon-black/polytetra-fluoroethylene electrodes have been manufactured.
- Remarkable activity of electro-Fenton process under neutral pH conditions.
- Significant ANT and TOC removal rates under moderate electrochemical conditions.
- High stability and durability of fabricated perovskite/CB/PTFE electrodes.

GRAPHICAL ABSTRACT
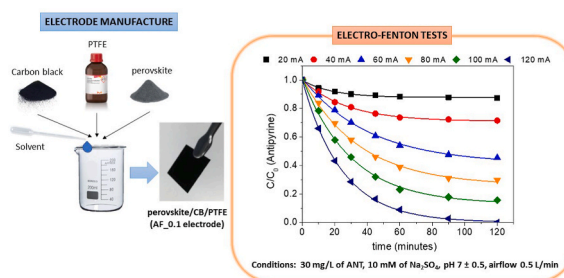
ARTICLE INFO

ABSTRACT

Bifunctional perovskite/carbon-black(CB)/polytetrafluoroethylene(PTFE) electrodes for electro-generation and catalytic decomposition of hydrogen peroxide to oxidizing hydroxyl radicals have been fabricated. These electrodes were tested for electroFenton (EF) removal of antipyrine (ANT) as a model antipyretic and analgesic drug. The influence of the binder loading (20 and 40 wt % PTFE) and type of solvent (1,3-dipropanediol and water) was studied for the preparation of CB/PTFE electrodes. The electrode prepared with 20 wt % PTFE and water exhibited a low impedance and remarkable H_2O_2 electro-generation (about 1 g/L after 240 min, a production rate of ca. 6.5 mg/h·cm^2). The incorporation of perovskite on CB/PTFE electrodes was also studied following two different methods: i) direct deposition on the CB/PTFE electrode surface and ii) addition in the own CB/PTFE/water paste used for the fabrication. Physicochemical and electrochemical characterization techniques were used for the electrode's characterization. The dispersion of perovskite particles in the own electrode matrix (method ii) exhibited a higher EF performance than the immobilisation onto the electrode surface (method i). EF experiments at 40 mA/cm^2 and pH 7 (non-acidified conditions) showed ANT and TOC removals of 30% and 17%, respectively. The increase of current intensity up to 120 mA/cm^2 achieved the complete removal of ANT and 92% of TOC mineralisation in 240 min. The bifunctional electrode also proved high stability and durability after 15 h of operation.

---

* Corresponding author.
** Corresponding author.
E-mail addresses: fernando.castillejo@urjc.es (F. Martínez), sanroman@uvigo.es (M.A. Sanromán).

1. Introduction

Electro-Fenton (EF) as an electrochemical advanced oxidation process is an effective, versatile, and ecological technology for removing toxic and persistent pollutants, which are refractory to conventional wastewater treatments (Poza-Nogueiras et al., 2018; Oturan and Aaron, 2014). This process is based on the electrochemical generation of hydrogen peroxide by oxygen reduction at the cathode, followed by its decomposition into hydroxyl radicals by the action of a redox Fenton-like catalyst. Additionally, the performance of EF processes can be enhanced through the adsorbed hydroxyl radicals generated on the anode surface by water oxidation (Brillas and Martínez-Huitle, 2015). Hydroxyl radicals are a powerful oxidant with $E°$ ($HO^\bullet/H_2O$) = 2.8 V to standard hydrogen electrode (Poza-Nogueiras et al., 2018; Oturan and Aaron, 2014). The *in-situ* electro-generation of hydrogen peroxide provides to EF systems remarkable economic and security advantages compared to the conventional Fenton process.

The research on EF processes has been generally focused on homogeneous catalysts, such as iron salts at a pH range of 2.8–3.5 (Ganiyu et al., 2018). However, the dissolved active catalysts present considerable disadvantages, such as the limited range of acid pH for an effective performance and the formation of a metallic sludge after neutralization. Both issues are currently limiting the potential use of EF technology for real application in wastewater treatment at the industrial level scale. In this context, the use of solid catalysts can overtake these weaknesses making easier the recovery of the catalytic material either for its reuse or use in continuous treatments (Monteil et al., 2018; Casado, 2019). Numerous works have reported the feasibility of powder catalysts in heterogeneous EF systems working in a broad range of pH (3–9) using iron oxides (magnetite, goethite, hematite, pyrite, and chalcopyrite) (Droguett et al., 2020; Ouriemmi et al., 2017; Wang et al., 2021; Puga et al., 2020), non-stoichiometric mixed oxides as perovskites (del Álamo et al., 2020; Ben Hammouda et al., 2019), zeolites (Ahmadi Zahrani and Ayati, 2020; Rostamizadeh et al., 2018), or MOFs (Ye et al., 2020; Yang et al., 2020).

Despite the promising activity and stability of powder catalysts, some of the latest works in this field have been addressed to the development of bifunctional electrodes with electroactive properties for H_2O_2 generation and catalytic activity to trigger Fenton reactions (Ganiyu et al., 2018; Garrido-Ramírez et al., 2016; Jiang et al., 2016). The manufacture of bifunctional cathodes is mainly based on the incorporation of active catalytic phases onto different types of conductive supports, such as metallic macroscopic structures (Choe et al., 2021; Do et al., 2017; Bocos et al., 2016a), or MOFs (Dong et al., 2021) and carbonaceous materials (Huong Le et al., 2019; Liu et al., 2018). However, carbonaceous materials, including graphite, carbon felts/clothes/fibres or carbon blacks, have been reported the most suitable ones as they gather the most favorable characteristics for their application in electrochemical systems (high conductivity, commercial availability, low-cost and sustainability) (Pérez et al., 2017).

Electrodes based on carbonaceous materials has normally used polytetrafluoroethylene (PTFE) as binder due to the exceptional chemical and thermal resistance, which make it very useful in the fabrication of electrodes for energy storage, microbial fuel cells, electrooxidation and capacitors. Furthermore, PTFE has provided a high chemical and mechanical stability (Imam Maarof et al., 2017), leading to low-cost electrodes with a high reproducible performance as compared to other binders such as Nafion (Dong et al., 2012), as well as excellent H_2O_2 generation rates (Pérez et al., 2017; García-Rodríguez et al., 2016).

This work has been focused on the preparation of catalytic active EF cathodes by the incorporation of crystalline perovskite particles. The electrode itself was fabricated based on a home-made method using carbon black and PTFE as main components. $LaCu_{0.5}Mn_{0.5}O_3$ perovskite was used according to its remarkable activity and stability in electro-Fenton (Cruz del Álamo et al., 2021) and Fenton (del Álamo et al., 2020) processes as powder material (del Álamo et al., 2020; Cruz del

Álamo et al., 2021). In the fabrication of perovskite/carbon black/PTFE electrodes, three different objectives were tackled in order to establish an optimum procedure for future manufacture of active EF electrodes: i) the binder amount in the electrochemical properties of the electrode, ii) the replacement of 1,3-dipropanediol commonly used in electrodes' preparation with PTFE by only water as a green solvent, and iii) the incorporation of the catalytic active perovskite material following two different methods based on superficial deposition or direct incorporation in the formulated composition of the electrode. Antipyrine (ANT) was chosen as model pollutant to assess the catalytic activity of the electrodes under different conditions and their potential application in a real wastewater treatment. ANT is an antipyretic and analgesic drug detected at average mass loads lower than 10 mg/day/1000 inhabitants in the effluents of wastewater treatment plants, with a relatively moderate removal efficiency (45% average) (Bedia et al., 2018).

2. Materials and methods

2.1. Materials

Metallic sources ($Cu(CH_3COO)_2 \cdot 2H_2O$, $Mn(NO_3)_2 \cdot 4H_2O$, La $(NO_3)_3 \cdot 6H_2O$) and citric acid for the synthesis of the powdered perovskite material were purchased from Sigma Aldrich. Carbon mesoporous nano-powder graphitized (so-called carbon black; CB), polytetrafluoroethylene (PTFE, 60 wt % dispersion in H_2O) and 1,3-dipropanediol for the preparation of carbon black/perovskite/PTFE electrodes were obtained from Sigma-Aldrich. Antipyrine, ANT, used as a model pollutant in the catalytic experiments, was also purchased from Sigma-Aldrich; and sodium sulfate (used as electrolyte) from ITW Reagents. High-performance liquid chromatography (HPLC) mobile phases were prepared with acetonitrile HPLC grade from Sigma-Aldrich and acetic acid glacial (99.7% purity) HPLC grade from Fisher Scientific. All solutions were prepared using Milli-Q grade ultrapure water.

2.2. Preparation and characterization of bifunctional perovskite/carbon-based electrodes

Synthesis of powder $LaCu_{0.5}Mn_{0.5}O_3$ perovskite. This material was prepared using the co-precipitation method described by Cruz del Álamo et al. (del Álamo et al., 2020) (more details are also included the in supporting information).

Preparation and electrochemical characterization of CB/PTFE electrodes. Electrodes were prepared according to the method described by Maarof et al. (Imam Maarof et al., 2017) based on the mixture of CB, PTFE solution (60 wt % in water) as organic binder and a solvent, but evaluating different PTFE mass percentages (20 and 40 wt %), and solvents (1,3-dipropanediol (DPD) or water (W)) to produce different viscous pastes. Those pastes were hand-pressed by aluminium foils to produce shaped rectangular flat-plate electrodes of 1.3 cm^2 (1.3 cm × 1 cm) and 2 mm thickness. CB/PTFE electrodes were coded according to the PTFE percentage and type of solvent, such as CB/PTFE_20_W (PTFE solution of 20 wt % and water as solvent). The electrodes were dried at different temperatures in three consecutive steps: 80 °C for 2 h, 125 °C for 1 h and, 250 °C for 1 h. After the thermal process, electrodes were hand-pressed again to improve the mechanical strength. Hydrogen peroxide production tests were performed to select the most appropriate formulation (PTFE mass percentage and solvent) for the further preparation of perovskite/CB/PTFE catalytic electrodes. Experiments were performed in the absence of antipyrine in an undivided batch electrochemical chamber using a platinum wire as anode and 50 mL of a 10 mM Na_2SO_4 solution as electrolyte. The current density was fixed at 40 mA/cm^2 and supplied by a power source (Siglent SPD 3303C). Air was continuously bubbled in the chamber at 0.5 L/min.

Preparation of perovskite/CB/PTFE electrodes. The incorporation of the powdered perovskite material ($LaCu_{0.5}Mn_{0.5}O_3$) into the optimised CB/PTFE electrodes was conducted following two different

methods: i) superficial immobilisation (SI) of powdered perovskite and ii) addition in the formulation (AF) of the CB/PTFE paste for the preparation of the electrode. In the first case, powered perovskite was immobilised by direct contact over the CB/PTFE electrode before the thermal process at 80 °C. The perovskite content incorporated into the available surface of the carbon electrode (1.3 cm^2) was 0.02 g (perovskite/CB/PTFE_SI_0.02). In the second case, different amounts of powdered perovskite (0.1 and 0.2 g) were mixed with the CB and PTFE solution before the solvent addition and further conformation process (perovskite/CB/PTFE_AF_0.1 and perovskite/CB/PTFE_AF_0.2, respectively). All the perovskite/CB/PTFE electrodes were dried using the same procedure followed by the CB/PTFE electrodes.

2.2.1. Physicochemical and electrochemical characterization of perovskite/CB/PTFE electrodes

The physicochemical characterization of perovskite/CB/PTFE electrodes surface was performed by X-ray diffraction (XRD), Raman spectroscopy and scanning electron microscopy (SEM) combined with energy dispersive spectrometry (EDS) to illustrate the presence of crystalline perovskite particles and to determine the crystallinity and superficial distribution on the electrodes, respectively (more details are described in supporting information). Electrochemical studies were conducted at room temperature using an Autolab PGSTAT302 N potentiostat (Metrohm) controlled by NOVA 2.1 software. Cyclic voltammetry (CV) tests were carried out in a single glass cell of 100 mL with a three-electrode configuration, using the prepared perovskite/CB/PTFE electrode as working electrode and Pt wire and Ag/AgCl (3 M KCl) as counter and reference electrodes, respectively. The electrolyte solution (10 mM of Na$_2$SO$_4$ at pH 7) was placed in the glass-cell without magnetic stirring and aeration, and five cycles were carried out for each electrode without any clean step between them. Cyclic voltammetries of electrodes were carried out in absence and presence of hydrogen peroxide. The scan rate of all CV tests was 0.025 V/s with steps of 0.005 V, fixing the start point of CV in 0 V and upper and lower vertex potential in ± 2 V, respectively. In previous CV tests, electrochemical impedance spectroscopy (EIS) was carried out using the same setup and instrument working in the frequency range from 10^6 to 10 Hz with a 10-mV sinusoidal perturbation. EIS was used to investigate the electron/charge transfer resistance at the interface between the electrode surface and electrolyte (Mann et al., 2022).

2.2.2. Performance of bifunctional perovskite/CB/PTFE electrodes for the removal of antypirine

Catalytic EF tests. EF experiments were performed in an undivided batch electrochemical chamber working with two electrodes separated 2 cm. The anode was a Pt wire, and the prepared perovskite/CB/PTFE electrode worked as cathode. Both electrodes are actives with a low oxygen evolution potential (Comninellis, 1994; Feng et al., 2003), which should limit the anodic oxidation contribution in the overall electrochemical process. The cathodic submerged active area was 1 cm^2. A direct current between 20 and 120 mA was constantly supplied by a power source (Siglent SPD 3303C), in which the voltage was monitored during operation. In a typical run, 50 mL of an antipyrine (ANT) solution (30 mg/L) containing 10 mM of Na$_2$SO$_4$ was placed in the reactor's chamber, keeping the natural pH of the initial solution (ca. 7 ± 0.5). Air was continuously bubbled in the chamber with an airflow of 0.5 L/min. The zero time for the electro-catalytic run was taken once the power supply was turned on. In all the cases, the electrochemical reactor operated at room temperature (22 ± 5 °C).

Specific energy consumption (EC) per mass unit of removed pollutant (ANT) was determined as shown in Eq. (1), where U is the applied cell voltage (V), I the average current intensity (A), t the time (h), V the solution volume (L) and $\Delta C_{pollutant}$ the difference in the ANT concentration (mg/L) before and after the reaction (Poza-Nogueiras et al., 2021). Moreover, the electrical energy consumption per mass unit of H$_2$O$_2$ electro-generated was also following the same equation

considering the term of concentration as H$_2$O$_2$.

$$EC \left(\frac{kWh}{g} \right) = \frac{U \cdot I \cdot t}{V \cdot \Delta C_{pollutant}} \tag{1}$$

Total Organic Carbon (TOC) was measured in a catalytic high-temperature combustion analyser (multi-N/C 3100 Autoanalyzer, Analytik Jena) coupled with a non-dispersive infrared detector (CACTI University of Vigo). The concentration of dissolved metals from the perovskite (La, Cu and Mn) after experiments in the aqueous samples was measured by inductively coupled plasma (ICP-OES) (CACTI, University of Vigo). ANT was determined by a HPLC (Agilent 1100) equipped with a Zorbax Eclipse XDB C8 (150 mm × 4.6 mm, i.d., 5 μm) column (Agilent) using a DAD detector at 242 nm. A solution composed of acetonitrile and 1.5% acetic acid (10:90 v/v) was used a as mobile phase with a flowrate of 1 mL/min. The column was kept at room temperature. Hydrogen peroxide concentration was determined following the titanium (IV) oxalate method using a GENESYS 150 UV–Vis Spectrophotometer (Sellers, 1980). All experiments were conducted in duplicate, and the concentration of the pharmaceutical pollutant was determined in duplicated, showing a standard deviation of <5%.

3. Results and discussion

3.1. Preparation of CB/PTFE electrode: influence of the binder loading and solvent

The first step for manufacturing conductive perovskite/CB/PTFE electrodes was to evaluate the influence of PTFE content as binder (20 and 40 wt %), and the use of 1,3-dipropanediol (DPD) or water (W) as solvent for the preparation of CB/PTFE electrodes. The organic DPD solvent is commonly used for the preparation of carbon-based electrodes (Imam Maarof et al., 2017), but water is employed for the first time as non-toxic and environmental-friendly solvent in the preparation of CB/PTFE electrodes.

Nyquist plots of electrochemical impedance spectroscopy (EIS) and hydrogen peroxide production for the CB/PTFE electrodes are shown in Fig. 1. Nyquist plots (Fig. 1a) displayed a semi-circular part at high frequencies and a long straight line with an angle of approximately 45° to the real axis at low frequencies, which evidenced a limited diffusion process (Dong et al., 2012; Kamyabi and Hajari, 2016). The diameter of the semicircular segment (depressed loop) is equivalent to the electron or charge transfer resistance (R$_{ct}$) (Bocos et al., 2016a), which indicates the kinetics of electron/charge transfer of the redox reactions at the electrode interface. Smaller R$_{ct}$ values typically reflect faster charge-transfer kinetics (Mann et al., 2022). The R$_{ct}$ values obtained for electrodes prepared with DPD were 137 and 114 Ω, whereas electrodes prepared with water were 83 and 143 Ω for 20 and 40% as mass percentage of PTFE, respectively. Results not showed significant differences, so it was not found a clear trend regarding the effect of PTFE loading and solvent on the preparation of CB/PTFE electrodes. Maarof et al. (Imam Maarof et al., 2017) also reported non-considerable variations in R$_{ct}$ values of three prepared electrodes of CB/PTFE using 20, 30 and 40% as mass percentage of binder, which is in accordance with the results obtained in this work. Interestingly, the CB/PTFE_20_W manufactured electrode showed the lowest R$_{ct}$ and consequently faster charge-transfer kinetics.

However, regarding the H$_2$O$_2$ production, the use of water as solvent for the preparation of electrodes significantly increased the production of the oxidant, accomplishing after 60 min values of 358 and 288 mg$_{H_2O_2}$/L for CB/PTFE_20_W and CB/PTFE_40_W, respectively, in comparison with 120 and 132 mg$_{H_2O_2}$/L when 1,3-dipropanediol was used (CB/PTFE_20_DPD and CB/PTFE_40_DPD, respectively). Interestingly, the CB/PTFE_20_W electrode prepared with water and the lower PTFE content (20 wt %) showed the highest hydrogen peroxide
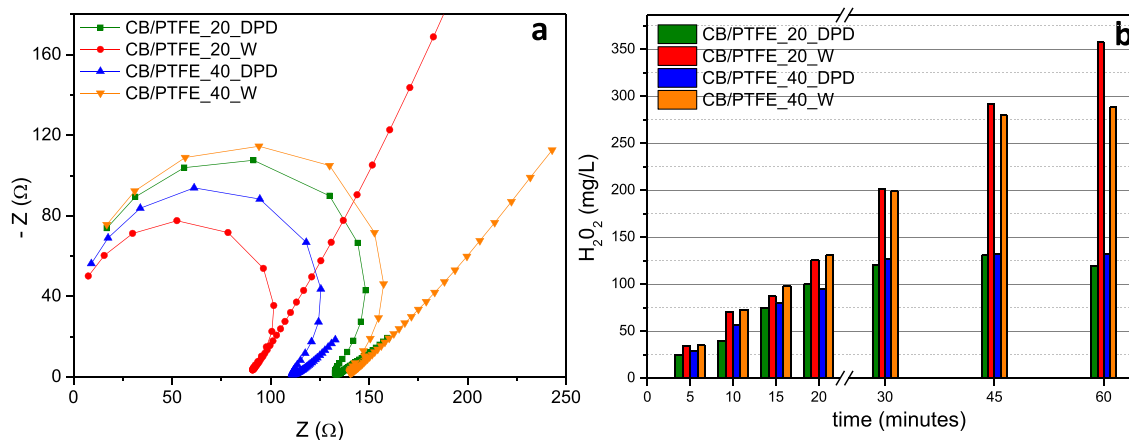
Fig. 1. (a) Nyquist plots of EIS and (b) hydrogen peroxide electro-generation (40 mA/cm^2 of current density, 10 mM of Na$_2$SO$_4$, pH ca. 7 $\pm$ 0.5 and airflow of 0.5 L/min) for different CB/PTFE electrodes.

production. This fact is in agreement with a higher content of carbon black, a more conductive and electro-active component for the H$_2$O$_2$ production, and a lower amount of PTFE which produced the main electron transfer resistance in the whole cathode (FangkeYu, 2021).

Thus, the CB/PTFE_20_W electrode evidenced the best results in terms of the electroreduction of oxygen to produce hydrogen peroxide and favorable electron/charge-transfer kinetics. Additionally, the H$_2$O$_2$ production for this electrode showed a linear increase up to ca. 3 h, with a production rate of 6.5 mg/h·cm^2 and a maximum concentration of ca. 1100 mg $_{H2O2}$/L after 5 h (Fig. S1). Values of 15 mg/h·cm^2 (Pérez et al., 2017) or 22 mg/h·cm^2 (Yu et al., 2015) have been reported for carbon felts modified by CB/PTFE. However, all those works used carbon cloths as carbon support for CB, which also has an active contribution to the H$_2$O$_2$ production between 0.4 and 2 mg/h·cm^2, as reported by Zou et al. (Zhou et al., 2014) and Fdez-Sanromán et al. (2020). The novelty of this work lies in the benefit of conforming individual CB/PTFE electrodes following an easy procedure without the necessity of an active support. Moreover, the substitution of 1,3-dipropanediol by water as solvent makes the CB/PTFE electrode preparation more environmentally sustainable, in contrast with other electrodes that use organic solvents (e.g., isopropanol (Pérez et al., 2017), 1,3-dipropanediol (Imam Maarof et al., 2017), ethanol (Dong et al., 2012) or *n*-butanol (Yu et al., 2015)).

3.2. Physico-chemical and electrochemical characterization of perovskite/CB/PTFE electrodes

The CB/PTFE_20_W electrode prepared with water and 20 wt % of PTFE was used for the incorporation of perovskite by direct deposition over the CB/PTFE electrode surface or the addition in the own perovskite/CB/PTFE paste for preparation of the electrode. XRD patterns of powdered CB/PTFE_20_W and perovskite/CB/PTFE electrodes after crushing evidenced PTFE characteristic diffraction peaks (Joseph et al., 2010) and two broad peaks corresponding to reflections of graphitized carbon (Chakrabarti et al., 2011; Lazzarini et al., 2016) for the CB/PTFE_20_W electrode and the characteristic perovskite signals of crystalline ABO$_3$ phase for perovskite/CB/PTFE electrodes (Fig. S2). In the case of the perovskite/CB/PTFE_SI_0.02 electrode, which contained the lowest amount of perovskite (ca. 10 wt %), the intensity of characteristic perovskite diffraction peaks decreased, and the main diffraction signals are attributed to PTFE and graphitized carbon. In contrast, the perovskite/CB/PTFE_AF_0.1 and perovskite/CB/PTFE_AF_0.2 electrodes showed the characteristic diffraction peaks of the crystalline perovskite material due to the higher mass percentage in these electrodes. The crystallinity of the carbon contained in the perovskite/CB/PTFE electrodes was also evaluated by Raman spectroscopy (Fig. S3). The

presence of perovskite into the CB/PTFE paste during the electrode preparation seems to promote a more ordered structure. This fact could be associated with a plausible rearrangement of the carbon layers of the carbon black during the thermal treatment of the electrode when the perovskite particles are present in the CB/PTFE matrix (Pawlyta et al., 2015).

SEM images of CB/PTFE electrode showed a smoother surface than perovskite/CB/PTFE electrodes (Fig. S4). The perovskite/CB/PTFE_SI_0.02 electrode prepared by superficial immobilisation of perovskite evidenced a rougher surface corresponding to the layer of perovskite particles deposited onto de CB/PTFE, whereas the perovskite/CB/PTFE_AF_0.1 and 0.2 electrodes prepared by incorporation of different amounts of perovskite in the own CB/PTFE paste for electrode fabrication displayed the presence of perovskite particles of different size (brighter zones) dispersed in the characteristic smooth surface of CB/PTFE electrode (darker zones) (del Álamo et al., 2020) (Chen et al., 2020).

Fig. 2 shows the elemental mapping analysis of manufactures electrodes (perovskite/CB/PTFE and perovskite-free CB/PTFE electrodes). The energy dispersive X-Ray spectroscopy (EDS) as superficial technique for chemical microanalysis, detected the emission of the six major elements on the electrode surface (carbon, lanthanum, fluorine, oxygen, copper, and manganese). Carbon represents the distribution of carbon black on the electrode surface, fluorine indicates the PTFE distribution and lanthanum is the main representative element of the perovskite material (Imam Maarof et al., 2017). Considering this, the CB/PTFE electrode only showed emissions for carbon, fluorine, and oxygen. Perovskite/CB/PTFE electrodes also emitted signals for La, Cu and Mn. Lanthanum dots, which represents the perovskite's presence, were well dispersed in the perovskite/CB/PTFE_SI_0.02 electrode, in which perovskite was immobilised superficially, whereas carbon emission is sparse. However, the red zones (carbon) become dominant in detriment of the orange zones (lanthanum) for the electrodes with the perovskite added to the CB and PTFE paste for preparation of the electrode (perovskite/CB/PTFE_AF_0.1 and 0.2). Likewise, the distribution of orange zones was more irregular for these electrodes. The quantitative composition of the surface electrode by EDS, considering the average of three different surface sites of each sample, is listed in Table S1. The superficial perovskite incorporation over the CB/PTFE electrode reduced the superficial carbon wt. % from ca. 69% in both perovskite/CB/PTFE_AF_0.1 and 0.2 electrodes, to 36% in the perovskite/CB/PTFE_SI_0.02 electrode. Carbon, as conductive element of the electrode, is necessary for the electro-generation of H$_2$O$_2$ over the electrode surface (reaction [R1]). However, the decrease of the superficial carbon is associated to the increase of active Cu and Mn species of
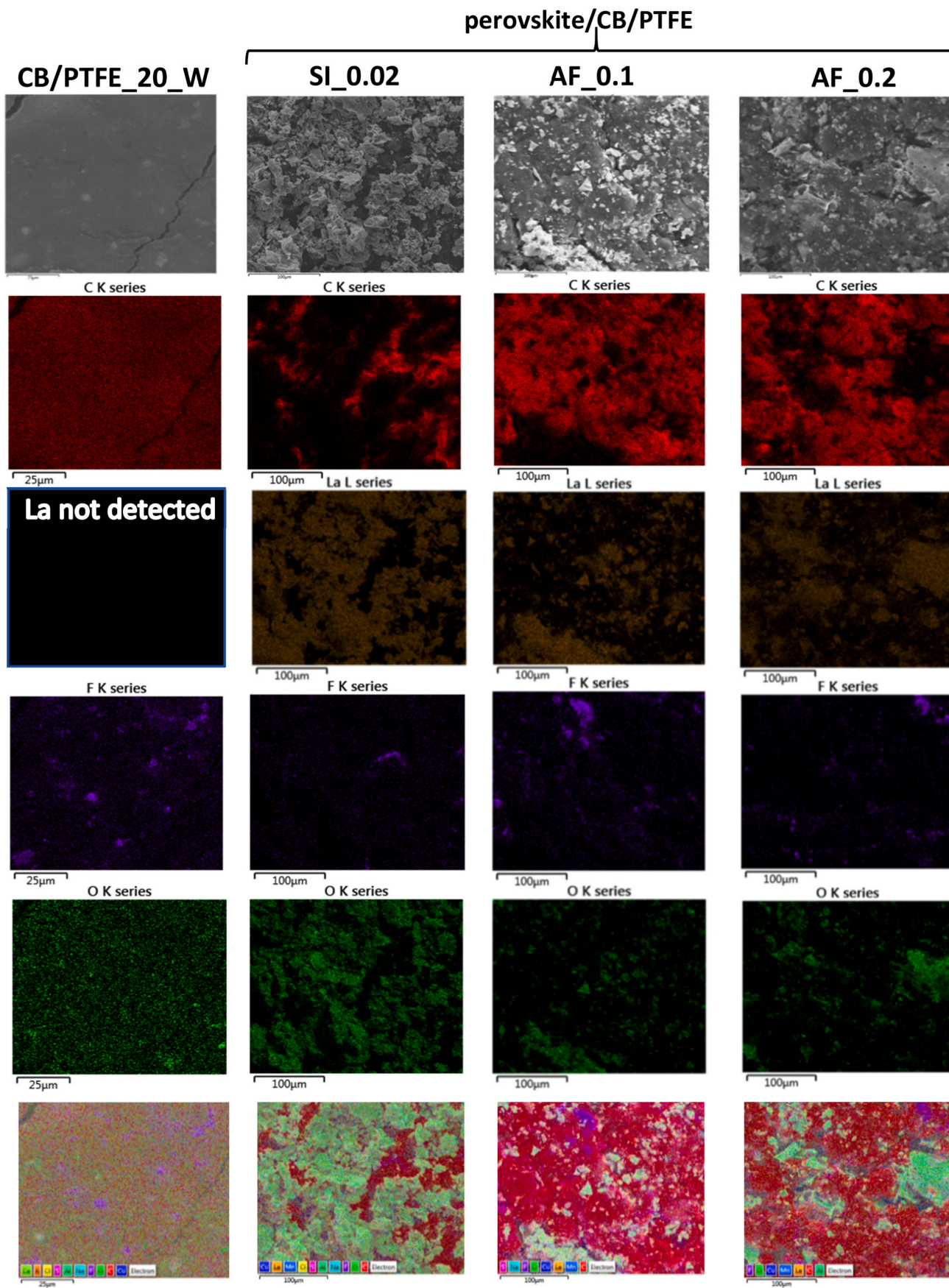
Fig. 2. FESEM-EDS elemental mapping of prepared perovskite/CB/PTFE electrodes.

perovskite particles in the Fenton reaction [R2] (see contents of La, Cu and Mn in Table S1), but in detriment of a necessary H_2O_2 electro-generation, which would limit the electro-Fenton process. Nevertheless, previous studies in Fenton systems have proved that Cu in perovskite materials is more active than Mn that seems to decompose inefficiently the H_2O_2 to H_2O and O_2 (Lu et al., 2018).

$$O_2 + 2H^+ + 2e^- \rightarrow H_2O_2 \qquad \text{[R1]}$$

$$M^n + H_2O_2 \rightarrow M^{n+1} + HO\cdot + HO^- \qquad \text{[R2]}$$

3.3. Electrochemical characterization of perovskite/CB/PTFE electrodes

Fig. 3 shows the electrochemical characterization of perovskite/CB/PTFE electrodes. Nyquist plots (Fig. S5) attaining R_{ct} values of 126, 115 and 127 Ω for perovskite/CB/PTFE_SI_0.02, AF_0.1 and AF_0.2 electrodes, respectively. EIS graphs demonstrated that the incorporation of a non-conductive perovskite material as catalyst in the electrode composition increased the electron/charge transfer resistance at the interface between the electrode surface and electrolyte, as the CB/PTFE electrode without perovskite exhibited a lower R_{ct} of 83 Ω. Moreover, the immobilisation of perovskite onto the surface of the electrode (perovskite/CB/PTFE_SI_0.02) promoted a higher impedance than the perovskite/CB/PTFE_AF_0.1 electrode with the perovskite incorporated in the bulk composition of the electrode. On the other hand, although the R_{ct} values of the three perovskite/CB/PTFE electrodes were not so different, it must be noted that the amount of non-conductive perovskite incorporated in perovskite/CB/PTFE_AF_0.1 and perovskite/CB/PTFE_AF_0.2 electrodes was about 5 and 10 times higher than the superficially supported in the perovskite/CB/PTFE_SI_0.02 electrode. Therefore, it was very relevant that the incorporation of a higher loading of non-conductive perovskite in the bulk composition of perovskite/CB/PTFE_AF_0.2 as compared to perovskite/CB/PTFE_AF_0.1 hardly increased the electrochemical resistance from 115 to 127 Ω, indicating the capacity of the CB/PTFE material to host the perovskite particles without affecting its electron conductivity significantly.

Cyclic voltammetry of CB/PTFE (Fig. 3a) and perovskite/CB/PTFE_SI_0.02, AF_0.1 and AF_0.2 (Fig. 3b, c and 3d, respectively) electrodes were carried out in: i) absence of hydrogen peroxide to evaluate the capacity of electrodes for oxygen reduction to generate hydrogen peroxide under continuous aeration, and ii) presence of hydrogen peroxide to assess the ability of active perovskite particles to decompose H_2O_2.

Regarding the CVs in absence of H_2O_2, the slope of the reduction line between −0.6 and −0.9 V evidenced a high electrochemical activity of the electrodes for the reduction of dissolved O_2 to generate H_2O_2 (according to the reaction: $O_2 + 2H^+ + 2e^- -> H_2O_2$) (Bocos et al., 2016b). The linear fitting of the slope was determined to assess the H_2O_2 electro-generation capacity of electrodes (supporting information, Fig. S6). A higher slope indicates an increase in the electrochemical capacity of the electrode to develop reactions that occur in the selected potential range (Domínguez et al., 2014). As expected, the CB/PTFE electrode without perovskite showed the highest electroactivity to generate H_2O_2 (slope value: $7.44 \cdot 10^{-3}$), due to its elevated presence of carbon and the absence of perovskite on the surface. The presence of perovskite in the electrode surface reduced the electrochemical capacity to produce H_2O_2, producing a considerable decrease for perovskite/CB/PTFE_SI_0.02 and perovskite/CB/PTFE_AF_0.2 with slope values of $6.6 \cdot 10^{-3}$ and $5.3 \cdot 10^{-3}$, respectively. However, the
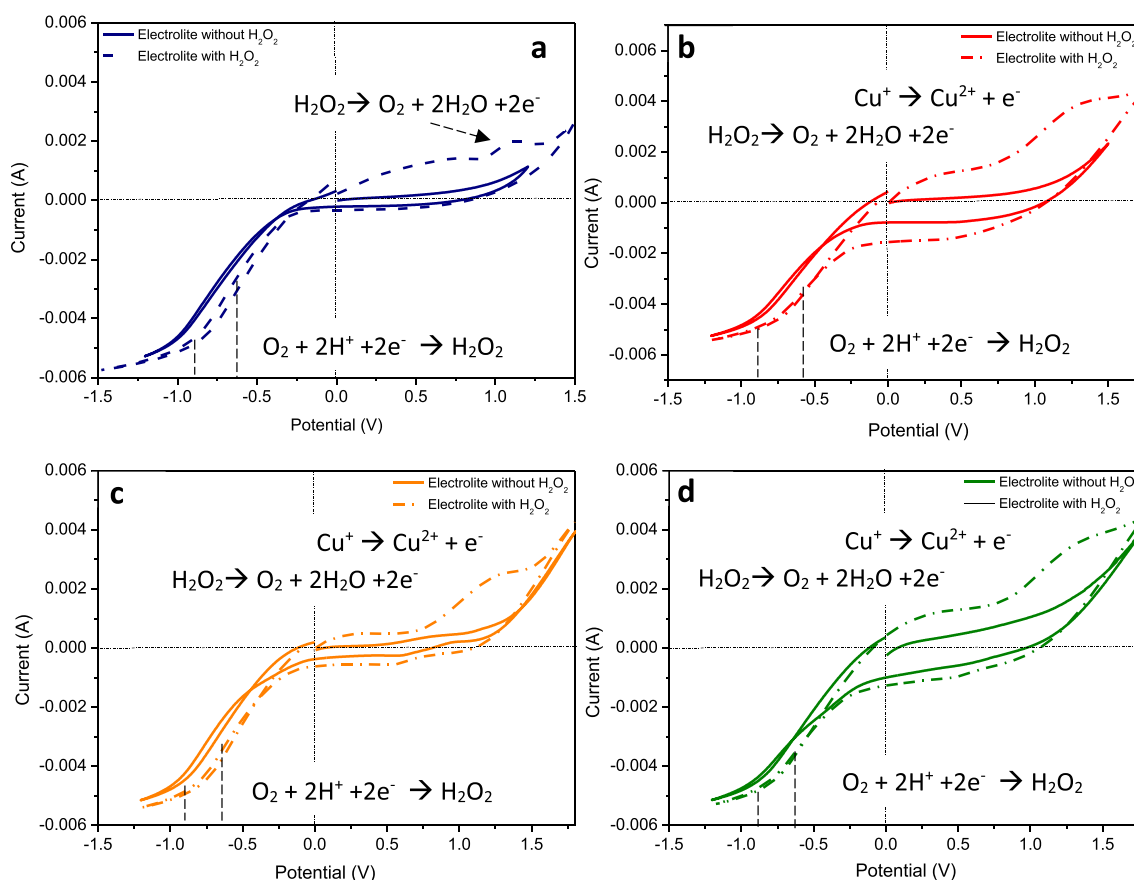

Fig. 3. Cyclic voltammograms of (a) CB/PTFE_20_W, (b) perovskite/CB/PTFE_SI_0.02, (c) perovskite/CB/PTFE_AF_0.1 and (d) perovskite/CB/PTFE_AF_0.2 at a voltage from 0 to ±2 V (scan rate: 0.025 V/s with steps of 0.005 V).

perovskite/CB/PTFE_AF_0.1 electrode displayed a similar electro-chemical capacity to CB/PTFE electrode ($7.1 \cdot 10^{-3}$ vs $7.44 \cdot 10^{-3}$ for perovskite/CB/PTFE_AF_0.1 and CB/PTFE_20_W- electrodes, respectively).

As previously mentioned, the behaviour of the electrode to decompose the H_2O_2 was also evaluated by adding H_2O_2 in the electrolyte. In this case, 350 mg/L H_2O_2 was added to detect a valued signal during tests. CV for CB/PTFE electrode showed an anodic peak at approximately 1–1.2 V, the voltage where the hydrogen peroxide can spontaneously decompose to water by the reaction $H_2O_2 \rightarrow O_2 + 2H_2O + 2e^-$ at pH 6–7 (J.L.T.R. Oscar Fabián Higuera Cobos, 2006). This anodic peak became broader in CV tests for perovskite/CB/PTFE because at this potential (c.a. 1.2 V), the oxidation of Cu (I) to Cu(II) also occurs (Jouda et al., 2018). Thus, these wider anodic peaks could be attributed to both reactions: (i) the decomposition of H_2O_2 and (ii) the oxidation of Cu (I) to Cu(II) present in the perovskite, which probably induces the peroxide decomposition into radical oxygen species (ROS).

3.4. Catalytic tests of perovskite/CB/PTFE catalytic electrodes

The activity of bifunctional electrodes for H_2O_2 production [R1] and catalytic decomposition of H_2O_2 into hydroxyl radicals through an electro-Fenton-like process [R2] were tested for the removal of ANT (30 mg/L) in an ultra-pure water matrix with 10 mM of Na_2SO_4, natural pH of the initial solution ca. 7 ± 0.5 and airflow of 0.5 L/min. Fig. 4a shows the ANT removal along the reaction time for all the prepared perovskite/CB/PTFE electrodes as well as the commercial graphite laminate and carbon felt electrodes, and the prepared CB/PTFE_20_W alone and with powder perovskite particles in slurry. The results of TOC mineralisation for all the experiments are shown in Fig. S7a. All the experiments were performed with a current density of 40 mA/cm^2.

The perovskite/CB/PTFE electrodes improved the performance of the CB/PTFE_20_W electrode. The highest ANT removal after 120 min was achieved by the perovskite/CB/PTFE_AF_0.1 electrode (28%) followed by electrode perovskite/CB/PTFE_AF_0.2 (23%) and perovskite/CB/PTFE_SI_0.02 (15%). Likewise, similar tendency was observed for the TOC mineralisation (Fig. S7a; 17, 14 and 8%, for the above-mentioned electrodes, respectively). At the same operation conditions, the CB/PTFE_20_W electrode in absence of the perovskite catalyst achieved ca. 10% and 4% of ANT removal and TOC mineralisation at 40 mA/cm^2, respectively. These results revealed a certain contribution of the anodic oxidation and radical oxygen species from sulfate anions (electrolyte) or CB/PTFE_20_W electrode through potential EF reactions. Interestingly, it was also noteworthy a higher activity of the CB/

PTFE_20_W than the other carbon electrodes employed in literature (graphite laminate and carbon felt) (Poza-Nogueiras et al., 2021; Fdez-Sanromán et al., 2021; Puga et al., 2021; Meijide et al., 2021).

Concerning the different performance of the perovskite/CB/PTFE electrodes, the lowest removal rate of the perovskite/CB/PTFE_SI_0.02 electrode (perovskite immobilised on the surface) was attributed to the low presence of carbon on the electrode surface, which is covered by the perovskite material in a large extension. Quantitative determination by EDS evidenced a low mass percentage of carbon on the surface of perovskite/CB/PTFE_SI_0.02 electrode (36%, Table S1) as compared to the others. This indicates the influence of the lower superficial amount of carbon, which seems to interfere in the H_2O_2 production, limiting the EF process. On the other hand, the enhanced catalytic performance of perovskite/CB/PTFE_AF_0.1 and perovskite/CB/PTFE_AF_0.2 electrodes is probably due to a higher CB/PTFE area on the electrode surface available for the oxygen saturated aqueous solution to produce hydrogen peroxide. The lower efficiency of the perovskite/CB/PTFE_AF_0.2 electrode could be attributed to the higher perovskite loading, as the non-conductive perovskite particles increased the electron/charge transfer resistance (see Fig. S5). This fact would affect the electro-generation rate of hydrogen peroxide on the electrode. Therefore, it is evident the critical point of finding a balance between enough H_2O_2 electro-generation [R1] and catalytic activity of metal phases for Fenton-like reactions [R2] to develop a high-efficient bifunctional electrode to perform a heterogeneous electro-Fenton process. In this work, the better compromise between these factors was achieved by the perovskite/CB/PTFE_AF_0.1 electrode. Likewise, it must be pointed out the low leaching of active metals from perovskite particles in the aqueous phase after the reaction time (0.001 mg$_{Mn}$/L and <0.010 mg$_{Cu}$/L), which proved the chemical stability of the bifunctional perovskite/CB/PTFE_AF_0.1 electrode. Finally, looking at the results of the control experiment conducted with the CB/PTFE_20_W electrode and the powdered perovskite in slurry (2 g/L, ca. the same concentration of the experiment performed with perovskite/CB/PTFE_AF_0.1 electrode), it was seen a lower ANT removal rate and TOC mineralisation for the perovskite catalyst in slurry. These results indicated that the performance of the EF process can be enhanced when the active perovskite catalyst is immobilised in the electrode following a proper method.

3.5. Influence of current density on the performance of perovskite/CB/PTFE electrode

The performance of the perovskite/CB/PTFE_AF_0.1 electrode was also assessed at different current densities between 20 and 120 mA/cm^2
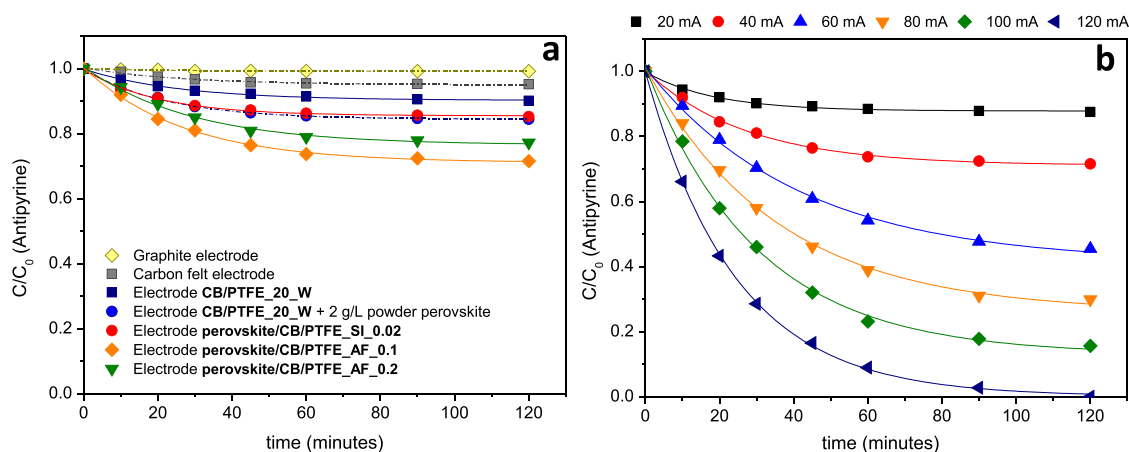

Fig. 4. ANT removal perovskite/CB/PTFE electrodes and control experiments at 40 mA/cm^2 (a) and perovskite/CB/PTFE_AF_0.1 at 20, 40, 60, 80, 100 and 120 mA/cm^2 (b) in an ultra-pure water matrix with ANT (30 mg/L), Na_2SO_4 (10 mM), natural pH of ca. 7 and airflow of 0.5 L/min.

keeping constant the rest of the operational conditions (30 mg/L of ANT, 10 mM of Na_2SO_4, pH 7 $\pm$ 0.5, airflow of 0.5 L/min). The profiles of ANT removal for 120 min are shown in Fig. 4b. The results clearly evidence that the rate of ANT removal increased with the current density, reaching a complete elimination at 120 min for 120 mA/cm^2. Likewise, TOC mineralisation (Fig. S7b) also exceedingly rose with the increment of current density, being necessary 240 min to accomplish almost complete mineralisation of ANT (92%). Additional control experiments were performed at the same current intensity (120 mA/cm^2) with the CB/PTFE_20_W, and other commercial carbon electrodes commonly used in literature, such as graphite laminate and carbon felt (Poza-Nogueiras et al., 2021; Fdez-Sanromán et al., 2021; Puga et al., 2021; Meijide et al., 2021). Negligible elimination rates of ANT and TOC mineralisation were observed for graphite laminate and carbon felt cathodes. In the case of CB/PTFE_20_W electrode, 23% of ANT removal and 13% TOC mineralisation after 120 min were achieved (Fig. S8). These results proved the important role of the perovskite/CB/PTFE_AF_0.1 electrode at higher current densities such as 120 mA/cm^2, which make more significant the differences between the EF system using the perovskite/CB/PTFE electrode (total ANT removal and 78% TOC mineralisation after 120 min; Fig. S8b) and the control experiment using the CB/PTFE electrode. Nevertheless, the results of CB/PTFE electrode also revealed the presence of parallel electro-oxidation processes that are contributing to the degradation of ANT in less extension.

The stability of the manufactured bifunctional electrode was also evaluated for the different current densities, considering the dissolution of potential active metals (Cu and Mn) in the reaction medium after reactions. For all the conditions, metal concentrations were very low. In the case of Cu, the concentration was below 0.010 mg/L working at 20, 40, 60 and 80 mA, and 0.035 and 0.081 mg/L at 100 and 120 mA, respectively. For Mn, the concentration was lower than 0.001 mg/L at 20, 40 and 60 mA, and 0.029, 0.033 and 0.064 mg/L at 80, 100 and 120 mA, respectively. Therefore, the perovskite/CB/PTFE electrode showed very promising results in terms of chemical stability along all the EF catalytic tests with a total operation time of 15 h as well as a remarkable enhancement of activity as the current intensity was increased.

The specific energy consumption (EC express per mass of removed ANT, kWh/g$_{ANT}$) of the process using the prepared bifunctional electrode as cathode (perovskite/CB/PTFE_AF_0.1) was calculated considering the highest intensity (120 mA), which provided a voltage of 27 V at 90 min. The specific energy consumption was 2.9 kWh/g$_{ANT}$ is still higher than that reported by the CB/PTFE/Ti electrode (0.95 kWh/g) (Poza-Nogueiras et al., 2021). However, it must be noted that in that work, CB was supported over a titanium metal electrode, reducing the electron transfer resistance in electro-Fenton reactor, and a BDD electrode was used as anode, which is a non-active electrode that has an important contribution in the partial oxidation of the contaminant by anodic oxidation. On the other hand, the specific EC for hydrogen peroxide production was calculated for the electrode without perovskite (CB/PTFE_20_W) using the optimum conditions of electro-generation achieved after 1 h at 40 mA (358 mgH$_2$O$_2$/L, Fig. 1b). The EC value was 0.020 kWh/gH$_2$O$_2$, also higher than others reported in literature for Vulcan CB/Pt or CB/PTFE/CarbonFelt electrodes reporting values of 0.006 kWh/g and 0.0032 kWh/g, respectively) (Karatas et al., 2022; Valim et al., 2013). EC and operation conditions of electrodes based on CB or PTFE electrodes are summarized in Table S2.

4. Conclusions

CB/PTFE electrodes using water as eco-friendly solvent and 20 wt % PTFE as binder have provided excellent electrochemical properties for application in electroFenton processes with favorable electron/charge-transfer kinetics and outstanding reduction of oxygen for H$_2$O$_2$ production. The incorporation of the active LaCu$_{0.5}$Mn$_{0.5}$O$_3$ perovskite particles in CB/PTFE electrodes by addition in the own preparation paste of the electrode was more effective. The immobilisation of perovskite as a layered material onto the CB/PTFE surface generated a higher electron/charge-transfer resistance. Electrochemical characterization of perovskite/CB/PTFE electrodes has proven the bifunctional role of perovskite/CB/PTFE electrodes for electro-generation of hydrogen peroxide and catalytic decomposition by the presence of active perovskite particles. A perovskite loading of 0.1 g in CB/PTFE electrodes provided an optimal balance between the oxidant production and its catalytic decomposition. This perovskite/CB/PTFE electrode showed remarkable results for ANT removal as model pollutant working between 40 and 120 mA/cm^2. The effectiveness of the electrode significantly improved with the increase of the current density. A complete elimination of ANT was achieved at 120 mA/cm^2 after 90 min and 78% of mineralisation after 140 min, being the energy consumption of the electro-Fenton reactor equal to 2.9 kWh/g$_{ANT}$ at these conditions. The concentrations of active metal ions of perovskite material in the aqueous solution after electroFenton reactions were almost negligible, revealing a high stability of the bifunctional perovskite/CB/PTFE electrodes for 15 h of operation working up to 120 mA/cm^2. The obtained results represent a significant progress in the manufacture of active EF cathodes non-supported on metallic or carbonaceous commercial electrodes following a method free of organic solvents. However, further studies are needed to offer an electrode manufacturing procedure that allows its scaling-up to an industrial level as well as its application in the treatment of real wastewater.

Author contribution statement

A. Cruz del Álamo: Conceptualization, Data curation, Formal analysis, Funding acquisition, Investigation, Methodology, Supervision, Writing – original draft, Writing – review & editing, **A. Puga:** Data curation, Formal analysis, Investigation, Methodology, **M.I. Pariente:** Supervision, Validation, Writing – review & editing, **E. Rosales:** Methodology, Supervision, Validation, Writing – review & editing, **R. Molina:** Supervision, Validation, Visualization, Writing – review & editing, **M. Pazos:** Methodology, Supervision, Validation, Funding acquisition, Writing – review & editing, **F. Martínez:** Supervision, Validation, Visualization, Funding acquisition, Writing – review & editing, **M.A. Sanromán**: Methodology' Supervision, Validation, Visualization, Funding acquisition, Writing – review & editing.

Declaration of competing interest

The authors declare that they have no known competing financial interests or personal relationships that could have appeared to influence the work reported in this paper.

Data availability

Data will be made available on request.

Acknowledgements

Appendix A. Supplementary data

Supplementary data to this article can be found online at https://doi.org/10.1016/j.chemosphere.2023.138858.

References

Ahmadi Zahrani, A., Ayati, B., 2020. Using heterogeneous Fe-ZSM-5 nanocatalyst to improve the electro Fenton process for acid blue 25 removal in a novel reactor with orbiting electrodes. J. Electroanal. Chem. 873, 114456 https://doi.org/10.1016/j.jelechem.2020.114456.

Bedia, J., Belver, C., Ponce, S., Rodriguez, J., Rodriguez, J.J., 2018. Adsorption of antipyrine by activated carbons from FeCl3-activation of Tara gum. Chem. Eng. J. 333, 58–65. https://doi.org/10.1016/j.cej.2017.09.161.

Ben Hammouda, S., Salazar, C., Zhao, F., Ramasamy, D.L., Laklova, E., Iftekhar, S., Babu, I., Sillanpää, M., 2019. Efficient heterogeneous electro -Fenton incineration of a contaminant of emergent concern-cotinine- in aqueous medium using the magnetic double perovskite oxide Sr2FeCuO6 as a highly stable catalyst: degradation kinetics and oxidation products. Appl. Catal. B Environ. 240, 201–214. https://doi.org/10.1016/J.APCATB.2018.09.002.

Bocos, E., Pérez-Álvarez, D., Pazos, M., Rodríguez-Argüelles, M.C., Sanromán, M.Á., 2016a. Coated nickel foam electrode for the implementation of continuous electro-Fenton treatment. J. Chem. Technol. Biotechnol. 91, 685–692. https://doi.org/10.1002/jctb.4626.

Bocos, E., Iglesias, O., Pazos, M., Ángeles Sanromán, M., 2016b. Nickel foam a suitable alternative to increase the generation of Fenton's reagents. Process Saf. Environ. Protect. 101, 34–44. https://doi.org/10.1016/J.PSEP.2015.04.011.

Brillas, E., Martínez-Huitle, C.A., 2015. Decontamination of wastewaters containing synthetic organic dyes by electrochemical methods. An updated review. Appl. Catal. B: Environ. 166–167, 603–643. https://doi.org/10.1016/J.APCATB.2014.11.016.

Casado, J., 2019. Towards industrial implementation of Electro-Fenton and derived technologies for wastewater treatment: a review. J. Environ. Chem. Eng. https://doi.org/10.1016/j.jece.2018.102823.

Chakrabarti, A., Lu, J., Skrabutenas, J., Xiao, Z., Maguire, J., Hosmane, N., 2011. Conversion of carbon dioxide to few-layer graphene. J. Mater. Chem. 21, 9491–9493. https://doi.org/10.1039/C1JM11227A.

Chen, L., Zhang, Y., Ma, C., 2020. Perovskites SrxLa1-xMnyCo1-yO3-δ coated on Ti as stable non-noble anode for efficient electrocatalytic oxidation of organic wastewater containing ammonia nitrogen. Chem. Eng. J. 393, 124514 https://doi.org/10.1016/j.cej.2020.124514.

Choe, Y.J., Kim, J., Byun, J.Y., Kim, S.H., 2021. An electro-Fenton system with magnetite coated stainless steel mesh as cathode. Catal. Today 359, 16–22. https://doi.org/10.1016/j.cattod.2019.06.062.

Comninellis, C., 1994. Electrocatalysis in the electrochemical conversion/combustion of organic pollutants for waste water treatment. Electrochim. Acta 39, 1857–1862. https://doi.org/10.1016/0013-4686(94)85175-1.

Cruz del Álamo, A., Zou, R., Pariente, M.I., Molina, R., Martínez, F., Zhang, Y., 2021. Catalytic activity of LaCu0.5Mn0.5O3 perovskite at circumneutral/basic pH conditions in electro-Fenton processes. Catal. Today 361, 159–164. https://doi.org/10.1016/j.cattod.2020.03.027.

del Álamo, A.C., González, C., Pariente, M.I., Molina, R., Martínez, F., 2020. Fenton-like catalyst based on a reticulated porous perovskite material: activity and stability for the on-site removal of pharmaceutical micropollutans in a hospital wastewater. Chem. Eng. J. 401, 126113 https://doi.org/10.1016/j.cej.2020.126113.

Do, T.M., Byun, J.Y., Kim, S.H., 2017. An electro-Fenton system using magnetite coated metallic foams as cathode for dye degradation. Catal. Today 295, 48–55. https://doi.org/10.1016/j.cattod.2017.05.016.

Domínguez, C.M., Ocón, P., Quintanilla, A., Casas, J.A., Rodriguez, J.J., 2014. Graphite and carbon black materials as catalysts for wet peroxide oxidation. Appl. Catal. B Environ. 144, 599–606. https://doi.org/10.1016/J.APCATB.2013.07.069.

Dong, H., Yu, H., Wang, X., Zhou, Q., Feng, J., 2012. A novel structure of scalable air-cathode without Nafion and Pt by rolling activated carbon and PTFE as catalyst layer in microbial fuel cells. Water Res. 46, 5777–5787. https://doi.org/10.1016/J.WATRES.2012.08.005.

Dong, P., Wang, H., Liu, W., Wang, S., Wang, Y., Zhang, J., Lin, F., Wang, Y., Zhao, C., Duan, X., Wang, S., Sun, H., 2021. Quasi-MOF derivative-based electrode for efficient electro-Fenton oxidation. J. Hazard Mater. 401, 123423 https://doi.org/10.1016/j.jhazmat.2020.123423.

Droguett, C., Salazar, R., Brillas, E., Sirés, I., Carlesi, C., Marco, J.F., Thiam, A., 2020. Treatment of antibiotic cephalexin by heterogeneous electrochemical Fenton-based processes using chalcopyrite as sustainable catalyst. Sci. Total Environ. 740, 140154 https://doi.org/10.1016/j.scitotenv.2020.140154.

FangkeYu, S. Wang H. Ma, 2021. Co-catalysis of metal sulfides accelerating Fe2+/Fe3+ cycling for the removal of tetracycline in heterogeneous electro-Fenton using an novel rolled NPC/CB cathodes. Separ. Purif. Technol. 275, 119200 https://doi.org/10.1016/J.SEPPUR.2021.119200.

Fdez-Sanromán, A., Acevedo-García, V., Pazos, M., Sanromán, M.Á., Rosales, E., 2020. Iron-doped cathodes for electro-Fenton implementation: application for pymetrozine degradation. Electrochim. Acta 338, 135768. https://doi.org/10.1016/J.ELECTACTA.2020.135768.

Fdez-Sanromán, A., Martinez-Treinta, R., Pazos, M., Rosales, E., Sanromán, M.Á., 2021. Heterogeneous electro-fenton-like designs for the disposal of 2-phenylphenol from water. Appl. Sci. 11 https://doi.org/10.3390/app112412103.

Feng, C., Sugiura, N., Shimada, S., Maekawa, T., 2003. Development of a high performance electrochemical wastewater treatment system. J. Hazard Mater. 103, 65–78. https://doi.org/10.1016/S0304-3894(03)00222-X.

Ganiyu, S.O., Zhou, M., Martínez-Huitle, C.A., 2018. Heterogeneous electro-Fenton and photoelectro-Fenton processes: a critical review of fundamental principles and application for water/wastewater treatment. Appl. Catal. B Environ. 235, 103–129. https://doi.org/10.1016/J.APCATB.2018.04.044.

García-Rodríguez, O., Bañuelos, J.A., Rico-Zavala, A., Godínez, L.A., Rodríguez-Valadez, F.J., 2016. Electrocatalytic activity of three carbon materials for the in-situ production of hydrogen peroxide and its application to the electro-fenton heterogeneous process. Int. J. Chem. React. Eng. 14, 843–850. https://doi.org/10.1515/ijcre-2015-0115.

Garrido-Ramírez, E.G., Marco, J.F., Escalona, N., Ureta-Zañartu, M.S., 2016. Preparation and characterization of bimetallic Fe–Cu allophane nanoclays and their activity in the phenol oxidation by heterogeneous electro-Fenton reaction. Microporous Mesoporous Mater. 225, 303–311. https://doi.org/10.1016/j.micromeso.2016.01.013.

Huong Le, T.X., Drobek, M., Bechelany, M., Motuzas, J., Julbe, A., Cretin, M., 2019. Application of Fe-MFI zeolite catalyst in heterogeneous electro-Fenton process for water pollutants abatement. Microporous Mesoporous Mater. 278, 64–69. https://doi.org/10.1016/j.micromeso.2018.11.021.

Imam Maarof, H., Daud, W., Aroua, M., 2017. Effect of varying the amount of binder on the electrochemical characteristics of palm shell activated carbon. IOP Conf. Ser. Mater. Sci. Eng. 210, 12011 https://doi.org/10.1088/1757-899X/210/1/012011.

Jiang, J., Li, G., Li, Z., Zhang, X., Zhang, F., 2016. An Fe–Mn binary oxide (FMBO) modified electrode for effective electrochemical advanced oxidation at neutral pH. Electrochim. Acta 194, 104–109. https://doi.org/10.1016/j.electacta.2016.02.075.

J.L.T.R. Oscar Fabián Higuera Cobos, 2006. Estudio electroquímico de la reducción del peróxido de hidrógeno, Scientia et Technica, vol. 1, pp. 349–354. ISSN 0122-1701.

Joseph, T., Uma, S., Philip, J., Sebastian, M., 2010. Electrical and thermal properties of PTFE-Sr2ZnSi2O7 composites. J. Mater. Sci. Mater. Electron. 22, 1000–1009. https://doi.org/10.1007/s10854-010-0250-4.

Jouda, A., Abood, E., Mashloor, M., 2018. Copper metal at new CuO nanoparticles modified carbonpaste electrode: selective voltammetric determination. Nano Biomed. Eng. 10, 243–249. https://doi.org/10.5101/nbe.v10i3.p243-249.

Kamyabi, M., Hajari, N., 2016. Low potential and non-enzymatic hydrogen peroxide sensor based on copper oxide nanoparticle on activated pencil graphite electrode. J. Braz. Chem. Soc. 28, 808–818. https://doi.org/10.21577/0103-5053.20160232.

Karatas, O., Gengec, N.A., Gengec, E., Khataee, A., Kobya, M., 2022. High-performance carbon black electrode for oxygen reduction reaction and oxidation of atrazine by electro-Fenton process. Chemosphere 287, 132370. https://doi.org/10.1016/J.CHEMOSPHERE.2021.132370.

Lazzarini, A., Piovano, A., Pellegrini, R., Agostini, G., Rudić, S., Lamberti, C., Groppo, E., 2016. Graphitization of activated carbons: a molecular-level investigation by INS, drift, XRD and Raman techniques. Phys. Procedia 85, 20–26. https://doi.org/10.1016/J.PHPRO.2016.11.076.

Liu, D., Zhang, H., Wei, Y., Liu, B., Lin, Y., Li, G., Zhang, F., 2018. Enhanced degradation of ibuprofen by heterogeneous electro-Fenton at circumneutral pH. Chemosphere 209, 998–1006. https://doi.org/10.1016/j.chemosphere.2018.06.164.

Lu, S., Wang, G., Chen, S., Yu, H., Ye, F., Quan, X., 2018. Heterogeneous activation of peroxymonosulfate by LaCo1-xCuxO3 perovskites for degradation of organic pollutants. J. Hazard Mater. 353, 401–409. https://doi.org/10.1016/J.JHAZMAT.2018.04.021.

Mann, D.K., Díez, A.M., Xu, J., Lebedev, O.I., V Kolen'ko, Y., Shatruk, M., 2022. Polar layered intermetallic LaCo2P2 as a water oxidation electrocatalyst. ACS Appl. Mater. Interfaces 14, 14120–14128. https://doi.org/10.1021/acsami.1c19858.

Meijide, J., Dunlop, P.S.M., Pazos, M., Sanromán, M.A., 2021. Heterogeneous electro-fenton as "green" technology for pharmaceutical removal: a review. Catalysts 11. https://doi.org/10.3390/catal11010085.

Monteil, H., Péchaud, Y., Oturan, N., Oturan, M.A., 2018. A review on efficiency and cost effectiveness of electro- and bio-electro-Fenton processes: application to the treatment of pharmaceutical pollutants in water. Chem. Eng. J. https://doi.org/10.1016/j.cej.2018.07.179.

Oturan, M., Aaron, J.-J., 2014. Advanced oxidation processes in water/wastewater treatment: principles and applications. A Review. Crit. Rev. Environ. Sci. Technol. 44. https://doi.org/10.1080/10643389.2013.829765.

Ouiriemmi, I., Karrab, A., Oturan, N., Pazos, M., Rozales, E., Gadri, A., Sanromán, M.Á., Ammar, S., Oturan, M.A., 2017. Heterogeneous electro-Fenton using natural pyrite as solid catalyst for oxidative degradation of vanillic acid. J. Electroanal. Chem. 797, 69–77. https://doi.org/10.1016/j.jelechem.2017.05.028.

Pawlyta, M., Rouzaud, J.N., Duber, S., 2015. Raman microspectroscopy characterization of carbon blacks: spectral analysis and structural information. Carbon 84, 479–490. https://doi.org/10.1016/j.CARBON.2014.12.030.

Pérez, J.F., Sáez, C., Llanos, J., Cañizares, P., López, C., Rodrigo, M.A., 2017. Improving the efficiency of carbon cloth for the electrogeneration of H2O2: role of polytetrafluoroethylene and carbon black loading. Ind. Eng. Chem. Res. 56, 12588–12595. https://doi.org/10.1021/acs.iecr.7b02563.

Poza-Nogueiras, V., Rosales, E., Pazos, M., Sanromán, M.Á., 2018. Current advances and trends in electro-Fenton process using heterogeneous catalysts – a review. Chemosphere 201, 399–416. https://doi.org/10.1016/J.CHEMOSPHERE.2018.03.002.

Poza-Nogueiras, V., Moratalla, Á., Pazos, M., Sanromán, Á., Sáez, C., Rodrigo, M.A., 2021. Towards a more realistic heterogeneous electro-Fenton. J. Electroanal. Chem. 895, 115475 https://doi.org/10.1016/J.JELECHEM.2021.115475.

Puga, A., Rosales, E., Pazos, M., Sanromán, M.A., 2020. Prompt removal of antibiotic by adsorption/electro-Fenton degradation using an iron-doped perlite as heterogeneous

catalyst. Process Saf. Environ. Protect. 144, 100–110. https://doi.org/10.1016/j.psep.2020.07.021.

Puga, A., Pazos, M., Rosales, E., Sanromán, M.A., 2021. Electro-reversible adsorption as a versatile tool for the removal of diclofenac from wastewater. Chemosphere 280, 130778. https://doi.org/10.1016/J.CHEMOSPHERE.2021.130778.

Rostamizadeh, M., Jafarizad, A., Gharibian, S., 2018. High efficient decolorization of Reactive Red 120 azo dye over reusable Fe-ZSM-5 nanocatalyst in electro-Fenton reaction. Separ. Purif. Technol. 192, 340–347. https://doi.org/10.1016/j.seppur.2017.10.041.

Sellers, R.M., 1980. Spectrophotometric determination of hydrogen peroxide using potassium titanium(IV) oxalate. Analyst 105, 950–954. https://doi.org/10.1039/AN9800500950.

Valim, R.B., Reis, R.M., Castro, P.S., Lima, A.S., Rocha, R.S., Bertotti, M., Lanza, M.R.V., 2013. Electrogeneration of hydrogen peroxide in gas diffusion electrodes modified with tert-butyl-anthraquinone on carbon black support. Carbon 61, 236–244. https://doi.org/10.1016/J.CARBON.2013.04.100.

Wang, Z., Pi, L., Cui, J., Zhang, X., Liu, Y., Tang, D., Zhu, H., Mao, X., 2021. Heterogeneous Electro-Fenton system for efficient degradation of 2,4-DCP: dual activation of O2 for H2O2 generation and oxygen-defect cobalt ferrite catalysts. Separ. Purif. Technol. 255, 117731 https://doi.org/10.1016/j.seppur.2020.117731.

Yang, Y., Liu, Y., Fang, X., Miao, W., Chen, X., Sun, J., Ni, B.-J., Mao, S., 2020. Heterogeneous Electro-Fenton catalysis with HKUST-1-derived Cu@C decorated in 3D graphene network. Chemosphere 243, 125423. https://doi.org/10.1016/j.chemosphere.2019.125423.

Ye, Z., Padilla, J.A., Xuriguera, E., Brillas, E., Sirés, I., 2020. Magnetic MIL(Fe)-type MOF-derived N-doped nano-ZVI@C rods as heterogeneous catalyst for the electro-Fenton degradation of gemfibrozil in a complex aqueous matrix. Appl. Catal. B Environ. 266, 118604 https://doi.org/10.1016/j.apcatb.2020.118604.

Yu, F., Zhou, M., Yu, X., 2015. Cost-effective electro-Fenton using modified graphite felt that dramatically enhanced on H2O2 electro-generation without external aeration. Electrochim. Acta 163, 182–189. https://doi.org/10.1016/J.ELECTACTA.2015.02.166.

Zhou, L., Zhou, M., Hu, Z., Bi, Z., Serrano, K.G., 2014. Chemically modified graphite felt as an efficient cathode in electro-Fenton for p-nitrophenol degradation. Electrochim. Acta 140, 376–383. https://doi.org/10.1016/J.ELECTACTA.2014.04.090.